


Differential expression of cell-cell junction proteins in the testis, epididymis, and ductus deferens of domestic turkeys (*Meleagris gallopavo*) with white and yellow semen

L. Pardyak,* A. Kaminska,* M. Brzoskwinia,* A. Hejmej,* M. Kotula-Balak,† J. Jankowski,‡
A. Ciereszko,§ and B. Bilinska *,1

*Department of Endocrinology, Institute of Zoology and Biomedical Research, Faculty of Biology, Jagiellonian University, 30-387 Krakow, Poland; †University Centre of Veterinary Medicine, University of Agriculture in Krakow, 30-059 Krakow, Poland; ‡Department of Poultry Science, Faculty of Animal Bioengineering, University of Warmia and Mazury in Olsztyn, 10-957 Olsztyn, Poland; and §Department of Gamete and Embryo Biology, Institute of Animal Reproduction and Food Research, Polish Academy of Sciences, 10-243 Olsztyn, Poland

ABSTRACT Tight, adherens, and gap junctions are involved in the regulation of reproductive tissue function in male mammals. In birds, including domestic turkeys, intercellular interactions performed by junctional networks have not yet been studied. Furthermore, the cellular and molecular basis of yellow semen syndrome (YSS) in the turkey population remains poorly understood. Thus, the aim of the present study was 2-fold: first, to provide new information on the localization and expression of cell-cell junction proteins in the testis, epididymis, and ductus deferens of domestic turkeys and second, to compare expression of junctional protein genes between 2 turkey population, one that produces white normal semen (WNS) and the other that produces yellow abnormal semen. Expression of *occludin*, *zonula occludens-1 (ZO-1)*, *connexin 43 (Cx43)*, *N- and E-cadherin*, and *β-catenin* genes were investigated using 3 complementary techniques: quantitative real-time PCR, western blot, and immunohistochemistry. Compared to WNS testis, epididymis, and ductus deferens, YSS tissues exhibited downregulation of

occludin and *β-catenin* mRNA ($P < 0.05$) and protein ($P < 0.05$ and $P < 0.01$, respectively) and upregulation of *N- and E-cadherin* mRNA ($P < 0.001$, $P < 0.05$, $P < 0.01$, respectively) and protein ($P < 0.01$, $P < 0.05$, and $P < 0.05$, respectively). In contrast, *ZO-1* and *Cx43* mRNA and protein were upregulated in YSS testis ($P < 0.05$ and $P < 0.001$, respectively) but not in epididymis and ductus deferens; both mRNAs and proteins were downregulated ($P < 0.05$) compared to the respective WNS epididymis and ductus deferens. Altered staining intensity of immunoreactive proteins in YSS vs. WNS reproductive tissue sections confirmed the gene expression results. The present study is the first to demonstrate altered levels of junctional protein gene expression in reproductive tissues of male YSS turkeys. These findings may suggest that subtle changes in junctional protein expression affect the microenvironment in which spermatozoa develop and mature and thus may have an impact on the appearance of yellow semen in domestic turkeys.

Key words: cell-cell junctional proteins, testis-epididymis-ductus deferens, domestic turkey, yellow semen syndrome

2020 Poultry Science 99:555–566
<http://dx.doi.org/10.3382/ps/pez494>

INTRODUCTION

Yellow semen syndrome (YSS), endemic within domestic turkey populations, was detected as early as the 1980s by identification of seminal plasma with a yellow color and a high protein concentration (Thurston et al., 1982); the cellular and molecular basis of this syndrome has not been intensively studied and, therefore, remains poorly understood. Yellow semen is lower qual-

ity and when used for insemination leads to decreased fertility and hatchability compared to the white normal semen (WNS) that is produced by most turkeys (Hess and Thurston, 1984). Although the total number of sperm and percentage of motile spermatozoa do not differ between white and yellow semen (Hess et al., 1976; Slowinska et al., 2011), there are apparent abnormal spermatids and sperm with lower motility and hypertrophied epithelial cells in ductuli deferentes of YSS males (Hess et al., 1982; Thurston and Korn, 1997). Other differences relate to proteomic profiling of white and yellow seminal plasma (Slowinska et al., 2015).

We recently reported markedly increased expression of aromatase and altered androgen and estrogen

Received September 5, 2018.

Accepted August 10, 2019.

¹Corresponding author: barbara.bilinska@uj.edu.pl

© 2019 The Authors. Published by Elsevier on behalf of Poultry Science Association Inc.

This is an open access article under the CC BY-NC-ND license (<http://creativecommons.org/licenses/by-nc-nd/4.0/>).

concentrations in the testis, epididymis, and ductus deferens of YYS compared to WNS males (Pardyak et al., 2018). In many mammalian species, the balance between testosterone and estradiol is crucial for spermatogenesis, normal sperm maturation within the epididymis, and proper functioning of the ductus deferens (Sharpe, 1998; Hess et al., 2001; O'Donnell et al., 2001; Carreau and Hess, 2010). Besides endocrine regulation, local intercellular interactions, performed by complex junctional networks, are also involved in male mammalian reproductive tissue function (Mruk and Cheng, 2015; Hejmej and Bilinska, 2018). Cell-cell junctions, i.e., tight, adherens, and gap junctions, regulate paracellular transport, cell adhesion and maintenance of tissue integrity, and metabolic coupling between neighboring cells (Goossens and van Roy, 2005; Mruk and Cheng, 2010; Pointis et al., 2010). Analyses of junctional protein gene expression in turkey testis, epididymis, and ductus deferens may contribute new data that helps elucidate cellular and molecular differences between males with white and yellow semen.

In the turkey testis (Deviche et al., 2011), similar to that of other poultry species, rodents, and many other mammals, developing germ cells remain in close contact with Sertoli cells using dynamic junctional complexes that form the blood-testis barrier (BTB), composed of coexisting tight, adherens, and gap junctions (Pelletier, 1990; Mruk and Cheng, 2004; Kopera et al., 2010). As in mammals, the avian BTB divides the seminiferous epithelium into 2 compartments (adluminal and basal), separates advanced germ cells within the testis from the influence of the immune system, and allows Sertoli cells to provide a specific microenvironment in the adluminal compartment of the epithelium (Cheng and Mruk, 2002; Mruk and Cheng, 2015).

The turkey epididymis and ductus deferens are both lined with a pseudostratified columnar epithelium and are therefore morphologically similar (Hess et al., 1976). It is likely that as in the mammalian excurrent duct system, the turkey epididymal and ductal epithelial cells communicate with one another by specialized intercellular junctions that form the blood-epididymis barrier (BEB) (Cyr et al., 1995). The BEB regulates the microenvironment within the duct to allow for sperm maturation and sequesters autoantigenic spermatozoa from the immune system, while a blood-vas deferens barrier secludes spermatozoa during their transit to the exterior (Robaire and Viger, 1995; Cyr, 2011). Both the BTB and BEB create a unique anatomical, physiological, and immunological microenvironment for proper germ cell development into fully functional sperm (Mital et al., 2011).

Several rodent models have recently been proposed to study the role for tight junction proteins (e.g., claudins and occludin) for spermatogenesis completion and homeostasis maintenance within rat excurrent duct epithelia (Levy and Robaire, 1999; Wong and Cheng, 2005; Cyr et al., 2007). Studies on mice that lacked BTB proteins demonstrated that compromised BTB function resulted in reduced fertility (Cheng and Mruk,

2002; Mruk and Cheng, 2004, 2015; Kopera et al., 2010). The cadherin/catenin complex was described as important to support cell adhesion and integrity in the tissue epithelia (Rowlands et al., 2000), while gap junctions, formed by connexins (e.g., Cx43), were reported as involved in tissue homeostasis maintenance through direct intercellular communication (Saez et al., 2003). Compared with extensive studies on mammals, little work was performed on the cell-cell junctions in non-mammalian vertebrates (Bergmann et al., 1984; Izzo et al., 2006) and scarce information is available related to the presence and expression of intercellular junction proteins in the testis of domestic birds (Osman et al., 1980; Pelletier, 1990; Banerjee and Chaturvedi, 2018).

Since the network of cell-cell junctions provided by tight, adherens, and gap junctions coordinates cellular functions within reproductive tissues and whole organs in mammals, we selected the representative protein or the protein complex for each junctional type and aimed to evaluate the expression of occludin/zonula occludens-1 (ZO-1)-based tight junctions, cadherin/catenin-based adherens junctions, and connexin 43 (Cx43)-based gap junctions in the testis, epididymis, and ductus deferens of WNS and YSS turkeys.

As mentioned above, we previously showed that an augmented aromatization process and high estrogen levels are characteristic in the testis, epididymis, and ductus deferens of YSS turkeys (Pardyak et al., 2018). We hypothesized that these factors may act on Sertoli, germ, and secretory epithelial cells of the excurrent duct and induce changes in *occludin*, *ZO-1*, *Cx43*, *N-cadherin*, and *β -catenin* gene expression. These changes, in turn, may alter the luminal microenvironment, crucial for the functional maturation and protection of spermatozoa. If so, the YSS may rely, at least partly, on discrete alterations of intercellular junctions present between various cellular players involved in spermatogenesis and sperm maturation.

MATERIAL AND METHODS

Animals and Tissue Preparation

In all 38-wk-old domestic turkeys (*Meleagris gallopavo*) with WNS (n = 6) and with YSS (n = 6) were obtained from the Turkey's Testing Farm of the Department of Poultry Science (University of Warmia and Mazury in Olsztyn). Semen of male turkeys producing white and yellow semen was monitored to 37 wk of age (Slowinska et al., 2015) and criteria for white and yellow semen classification were used as described by Thurston et al. (1982). Semen with a white color and a low seminal plasma protein concentration (≤ 20 mg/mL) was classified as normal white whereas yellow-colored semen with a high seminal plasma protein concentration (> 20 mg/mL) was classified as abnormal yellow.

Fragments (0.5 cm \times 0.5 cm) of testes, epididymides, and ductuli deferentes of both populations of males were obtained immediately *post mortem*. The tissue samples were fixed in Bouin's fixative (saturated picric

Table 1. Sequences of forward and reverse primers.

Genes	Primers (5'–3')	Product size (bp)	Annealing temp. (°C)
occludin	5'- GAGCCCAGACTACCAAAGCAA-3'	68	55
	5'- GCTTGATGTGGAAGAGCTTGTTG-3'		
ZO-1	5'- CCGCAGTCGTTCCACGATCT-3'	63	54
	5'- GGAGAATGTCTGGAATGGTCTGA-3'		
Cx43	5'-GTCTTCATGCTGGTAGTGTCTTTGGTGT-3'	1558	61
	5'- CTGTGGGAGTAGGGGTCGGTTTTTC-3'		
N-cad	5'- GAATGGGACAGTTCCTGAAGGAT -3'	75	56
	5'- GCATCGATGGCAGTAACAGTCATTA -3'		
E-cad	5'- GACAGGGACATGAGGCAGAA -3'	120	54
	5'- GTACAACAACGACACAAATAG -3'		
B-cad	5'- ATGGCAATCAAGAAAGTAAGC-3'	61	52
	5'- AGCCAT CCCTCCTTCGCACA-3'		
β -actin	5'- AAGTACCCCATTTGAACACGG -3'	257	54
	5'- ATCACAATGCCAGTGGTACG -3'		

acid, formaldehyde, glacial acetic acid at 15:5:1 proportion) for 24 h, dehydrated in an increasing gradient of ethanol, and embedded in paraffin. After mounting on slides, all sections (5 μ m) were cleared in xylene, rehydrated in a series of ethanol grade, and washed in water (Slowinska et al., 2014; Bilinska et al., 2018). Other tissue fragments were frozen in liquid nitrogen and stored at -80°C for RNA isolation and protein extraction.

RNA Isolation and Reverse Transcription

Total RNA was extracted from testes, epididymides, and ductuli deferens (pooled after collection from the individual males) using TRIzol reagent (Life Technologies, Gaithersburg, MD, USA) as described by Pardyak et al. (2018). To remove contaminating DNA and the DNase from RNA preparations, the RNA samples were incubated with reagents from TURBO DNase free Kit (Ambion, Austin, TX, USA). The yield and quality of the RNA were assessed by measuring the A260:A280 ratio in a NanoDrop ND2000 Spectrophotometer (Thermo Scientific, Wilmington, DE, USA) and by electrophoresis. The purified total RNA was used to generate total cDNA. A volume equivalent to 1 μ g of total RNA was reverse transcribed using high-capacity cDNA Reverse Transcription Kit (Applied Biosystems, Carlsbad, CA, USA) according to the manufacturer’s protocol. Total cDNA was prepared in a 20 μ L volume using the random primers, dNTPmix, RNase inhibitor, and reverse transcriptase (RT). For a negative control, the same reactions without adding of RT were performed simultaneously (1 μ L of RNase-free water was added in place of RT). The RT+ and RT– samples then were subjected to PCR amplification performed in a Veriti Thermal Cycler (Applied Biosystems, Carlsbad, CA, USA).

Real-Time Quantitative RT-PCR

To determine alterations in *occludin*, *ZO-1*, *Cx43*, *N-* and *E-cadherin*, and β -*catenin* mRNA expression, quantitative real-time polymerase chain reaction (qPCR) analyses were performed.

Real-time RT-PCR was performed using the StepOne Real-Time PCR system (Applied Biosystems, Carlsbad, CA, USA) and optimized standard conditions as described in detail (Gorowska et al., 2014). Primer sets (Institute of Biochemistry and Biophysics, Polish Academy of Sciences, Warsaw, Poland) are listed in Table 1. Detection of amplification products for individual genes was performed with 10 ng cDNA, 0.5 mM primers, and SYBR Green master mix (Applied Biosystems, Carlsbad, CA, USA) in a final volume of 20 mL. Amplifications were performed as follows: 55°C for 2 min, 94°C for 10 min, followed by annealing temperature for 30 s (Table 1) and 45 s 72°C to determine the cycle threshold for quantitative measurement. To monitor DNA contamination, control reactions without the RNA template were performed in triplicate and one reaction without the RT enzyme was carried out per tissue sample.

Relative quantification (RQ) was obtained using the $2^{-\Delta\Delta C_t}$ method, adjusting the *occludin*, *ZO-1*, *Cx43*, *N-* and *E-cadherin*, and β -*catenin* mRNAs expression to the expression of β -*actin* mRNA. Relative levels of the transcripts in YSS testicular, epididymal, and ductal samples were compared with WNS values, which were arbitrarily set as 1 (RQ = 1) (Livak and Schmittgen, 2001).

Three independent experiments were performed, each in triplicate. All PCR products were analyzed by gel electrophoresis on 1.5 to 2.5% agarose gels with ethidium bromide together with a ready-to-load 100-bp DNA ladder marker (Promega, Southampton, UK) and followed by fluorescence digitization using a Bio-Rad Gel-Doc XR system (Bio-Rad Labs., Hercules, CA, USA).

Western Blot Analysis

Western blot analyses were performed to assess changes in the levels of *occludin*, *ZO-1*, *Cx43*, *N-* and *E-cadherin*, and β -*catenin* in YSS and WNS testes, epididymides, and ductuli deferentes.

Table 2. Primary antibodies used in this study.

Antibody	Host species	Vendor	Catalog no	Application(s)/dilution(s)
occludin	Rabbit	Invitrogen	71-1500	IHC (1:50) WB (1:500)
ZO-1	Rabbit	Invitrogen	61-7300	IHC (1:50) WB (1:500)
Cx43	Rabbit	Sigma-Aldrich	C6219	IHC (1:400) WB (1:8000)
N-cad	Mouse	Thermo Fisher	33-3900	IHC (1:50) WB (1:500)
E-cad	Rabbit	Invitrogen	PA5-19479	IHC (1:100) WB (1:1000)
β -cat	Rabbit	Invitrogen	71-2700	IHC (1:100) WB (1:1000)
β -actin	Mouse	Sigma-Aldrich	A2228	WB (1:3000)

First, the tissues collected from the individual males were pooled and samples of testes, epididymides and ductuli deferens were homogenized on ice with a cold Radio-Immuno-precipitation Assay Buffer (RIPA, pH 8.0; Thermo Scientific; Inc., Rocheford, IL, USA) supplemented with protease inhibitor cocktail (Sigma-Aldrich). Second, the tissue samples were sonicated and centrifuged at 10,000 g for 20 min at 4°C as described previously (Hejmej et al., 2012). Aliquots were assayed for protein by the Lowry dye-binding with bovine serum albumin as a standard (Bio-Rad Labs, GmbH, München, Germany). Next, 50 μ g of protein was solubilized in a sample buffer (Bio-Rad Labs) and heated at 99.9°C for 5 min. After denaturation, proteins were separated by SDS-PAGE in 6 to 10% (vol/vol) resolving gels under reducing conditions. Separated proteins were transferred on to polyvinylidene difluoride membranes (Merck Millipore, Darmstadt, Germany) using a wet blotter in the Genie Transfer Buffer (pH 8.4) for 90 min at a constant current of 250 mA. Nonspecific binding sites were blocked with a solution of non-fat dry milk (5%, wt/v) containing 0.1% Tween 20 (vol/vol), and the membrane was incubated with respective primary antibody against occludin, ZO-1, Cx43, N- and E-cadherin, and β -catenin (Table 2) at 4°C overnight. All primary antibodies were commercially available and recommended for chicken. Thereafter, the membranes were washed with TBS buffer with Tween 20 (0.05-M Tris-HCl, 0.15-M NaCl, pH 7.6 containing 0.1% Tween 20) and incubated in a goat anti-rabbit or horse anti-mouse IgG conjugated to horseradish peroxidase (1:3,000; Vector Labs, Burlingame, CA, USA) for 1 hr at room temperature. Immunoreactive proteins were detected using chemiluminescence with western blotting luminol reagent (Santa Cruz Biotechnology), and images were captured with a ChemiDoc™ XRS+ System (Bio-Rad Laboratories). All immunoblots were stripped with stripping buffer containing 62.5 mM Tris-HCl, 100 mM 2-mercaptoethanol and 2% SDS (wt/vol) (pH 6.7) at 50°C for 30 min, and incubated in an antibody against β -actin (dilution, 1: 3000; Sigma-Aldrich), which served as the loading control. The bands were densitometrically scanned using Image Lab™ 2.0 (Bio-Rad Labs) and the values obtained

for occludin, ZO-1, Cx43, N- and E-cadherin, and β -catenin were normalized against the corresponding β -actin. The molecular weights of target proteins were estimated by reference to standard proteins (Color-Burst Electrophoresis Marker, Sigma-Aldrich). Protein levels from WNS tissues were arbitrarily set as 1, against which statistical significance was analyzed.

Immunohistochemistry

To achieve antigen retrieval, slides were immersed in 10 mM citrate buffer (pH 6.0) and/or in Tris-EDTA buffer (10 mM Tris containing 1 mM EDTA and 0.05% Tween 20; pH 9.0), and heated for 3 to 5 min in a microwave oven (750 W) as described previously (Pardyak et al. (2018)). In brief, sections were incubated with the same antibodies as for western blotting (Table 2), at 4°C overnight. Subsequently, sections were incubated with biotinylated secondary antibody goat anti-rabbit or horse anti-mouse IgG (1: 500; Vector Labs). After each step of these procedures sections were rinsed with TBS. The staining was developed using avidin biotinylated horseradish peroxidase complex (ABC/HRP; 1:100; Vectastain Elite ABC Reagent, Vector Lab.) for 30 min. Bound antibody was visualized with TBS containing 0.05% 3,3'-diaminobenzidine tetrachloride (DAB; Sigma-Aldrich) and 0.07% imidazole for 4 to 5 min. Thereafter, sections were washed and counterstained with Mayer's hematoxylin, dehydrated and mounted using DPX mounting media (Sigma-Aldrich). To validate specificity of primary antibodies used for immunohistochemistry western blotting was performed (Bordeaux et al. 2010). Control sections included omission of the primary antibody and substitution by an irrelevant IgG. The sections were examined with a Leica DMR microscope (Leica, Microsystems GmbH Wetzlar, Wetzlar, Germany).

Qualitative and Quantitative Evaluation of the Immunohistochemical Reactions

Immunohistochemical staining for all antigens, occludin, ZO-1, Cx43, N- and E-cadherin, and β -catenin

was evaluated qualitatively in at least 20 serial sections from each tissue. The slides were processed immunohistochemically at the same time with the same treatment so that the staining intensities could be compared (Kotula-Balak et al., 2008). The tissue cells were considered immunopositive if brown reaction product was present at the testicular, epididymal, and ductal epithelia; the cells without any specific immunostaining were considered immunonegative. All immunohistochemical stainings were repeated at least 3 times.

For quantitative analysis of the staining intensity, digital color images of testis, epididymis, and ductus deferens sections were obtained using a CCD Video Camera (KYF55, JVC) mounted on an optical microscope (Microphot, Nikon, Japan) and connected to a video capture card (PV BT878P1, ProLink, Nei-Hu, Taipei, Taiwan) installed in a personal computer. Image processing and analyses were performed using ImageJ software (National Institutes of Health, Bethesda, MD, USA). The intensity of immunostainings was expressed as relative optical density of diaminobenzidine brown reaction products and calculated using the formula described by Smolen (1990). A total number of 60 tissue sections ($n = 10$ per tissue; a random selection of YSS and WNS tissue sections) were subjected to image analysis and results of 10 separate measurements were expressed as mean \pm SD.

Statistical Analysis

Each variable was tested using the Shapiro–Wilk W-test for normality. The homogeneity of variance was assessed with Levene’s test. All statistical analyses were performed using non-parametric Mann–Whitney U-test to determine which YSS values differed significantly from WNS values that served as controls. The analysis was made using Statistica 10 (Statsoft, Poland). Data were presented as mean \pm SD. Data were considered statistically significant at $P < 0.05$.

RESULTS

Expression of Occludin, ZO-1, N- and E-cadherin, β -catenin, and Cx43 mRNA in Turkey Reproductive Tissues

Electrophoresis revealed PCR-amplified products of the following predicted size: 68 base pairs (bp) for occludin, 63 bp for *ZO-1*, 1,558 bp for *Cx43*, 75 bp for *N-cadherin*, 120 bp for *E-cadherin*, 61 bp for β -catenin, and 257 bp for β -actin in YSS and WNS testes, epididymides, and ductuli deferentes (Figure 1A–E; see respective bands).

Quantitative real-time PCR analysis revealed down-regulation of *occludin* and β -catenin mRNA (Figure 1A and E) in all YSS tissues ($P < 0.05$), upregulation of *N-* and *E-cadherin* in YSS testis, epididymis, and ductus deferens ($P < 0.001$, $P < 0.05$, and $P < 0.01$, respec-

tively; Figure 1D), while *ZO-1* and *Cx43* mRNA were upregulated ($P < 0.05$ and $P < 0.001$, respectively) in YSS testis (Figure 1B and C) but not in epididymis and ductus deferens, in which both mRNAs were downregulated ($P < 0.05$; Figure 1B and C) compared to the respective WNS tissues (Figure 1A–E)

Expression of Occludin, ZO-1, N- and E-cadherin, β -catenin, and Cx43 Protein in Turkey Reproductive Tissues

Immunodetectable proteins were observed as single bands near 65 kDa (occludin), 210 kDa (*ZO-1*), 43 kDa (*Cx43*), 135 kDa (*N-* and *E-cadherin*), 92 kDa (β -catenin), and 42 kDa (β -actin) (Figure 1A’–E’; see respective bands). Protein band intensities were either markedly reduced or increased in YSS vs. WNS tissue samples as measured quantitatively.

Quantitative analysis of 3 separate experiments indicated that occludin and β -catenin expression decreased ($P < 0.05$; $P < 0.01$) and *N-* and *E-cadherin* increased ($P < 0.01$; $P < 0.05$) in all YSS tissues (Figure 1A’, D’, and E’) compared to the respective WNS tissues. *ZO-1* and *Cx43* protein levels, however, were elevated ($P < 0.05$ and $P < 0.001$, respectively) in YSS testis but not in the epididymis and ductus deferens (Figure 1B’ and C’). In the latter tissues, *ZO-1* ($P < 0.05$) and *Cx43* ($P < 0.01$) were significantly reduced compared to the respective WNS tissues (Figure 1B’ and C’).

Immunohistochemical Detection of Occludin, ZO-1, Cx43, N- and E Cadherin, and β -Catenin in Turkey Reproductive Tissues

Alterations in the localization and immunoexpression of junctional proteins were characterized using qualitative and quantitative analyses. Immunohistochemistry revealed positive staining for all examined junctional proteins in YSS and WNS testes, epididymides, and ductuli deferentes (Figures 2A–C and 3A–B). Detailed descriptions for each junctional protein are presented below.

Occludin and ZO-1 In YSS testis, occludin was delocalized between Sertoli and germ cells; the signal ran perpendicular to the basement membrane, exhibited “a spoke-like” pattern, and failed to localize to the BTB. Comparatively, in WNS testis, occludin signal ran parallel to the basement membrane, consistent with its localization at the BTB (Figure 2A). In YSS epididymis, occludin appeared as discontinuous lines at the BEB region. More precisely, this staining pattern was prominent at the apical-lateral border of the principal epithelial cells vs. continuous lines observed close to the luminal border of the WNS epididymal epithelium. Of note, this altered signal pattern was observed over the entire YSS epididymis length (Figure 2A; compare inserts at higher magnification). In YSS ductus deferens,

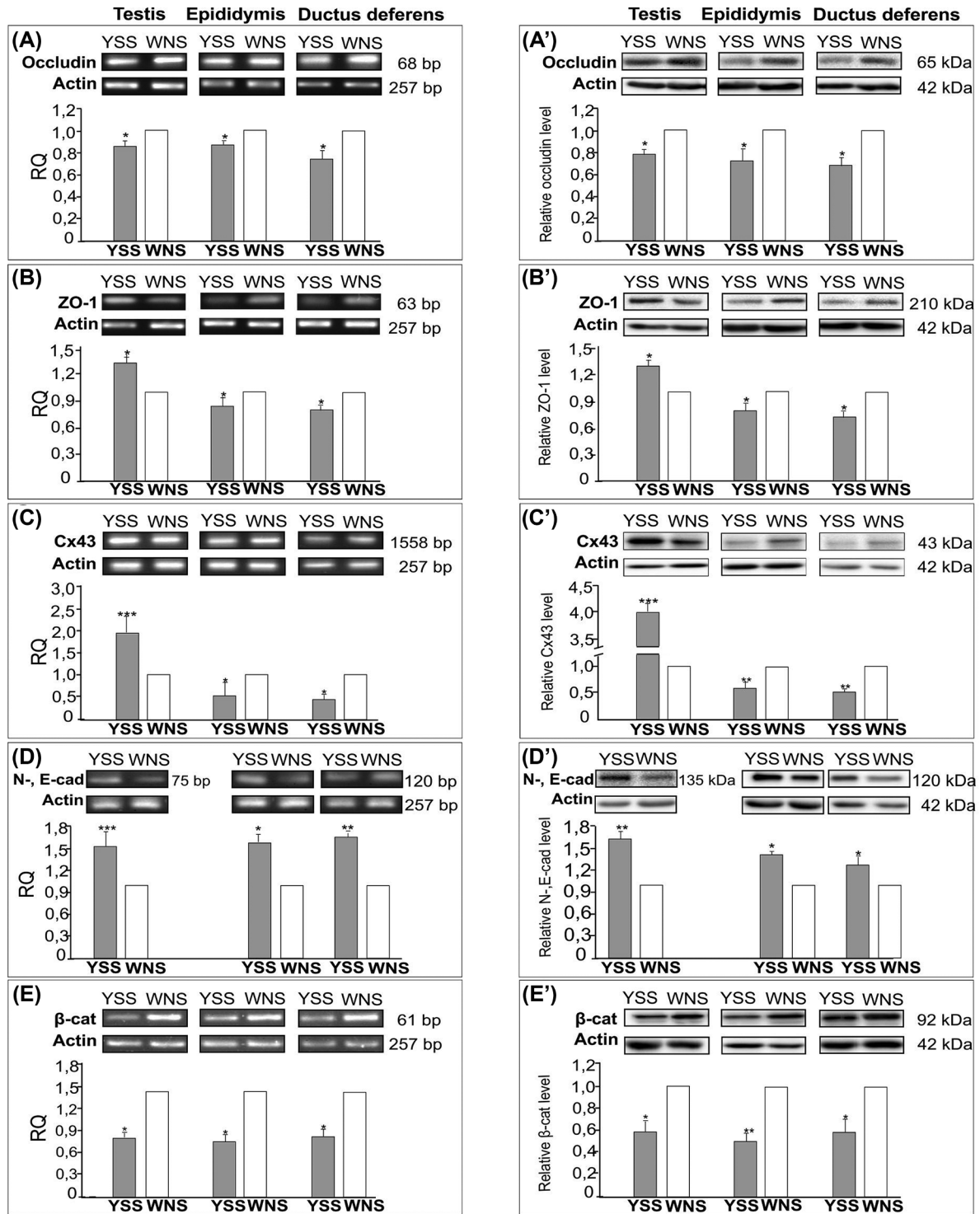


Figure 1. Occludin, ZO-1, Cx43, N- and E-cadherin, and β -catenin mRNA (A to E) and protein (A' to E') expression in yellow semen syndrome (YSS) and white normal semen (WNS) testes, epididymides, and ductuli deferentes. Representative quantitative real-time PCR analysis of *occludin* (A), *ZO-1* (B), *Cx43* (C), *N-* and *E-cadherin* (D), and *β -catenin* (E) mRNA expression in YSS and WNS testes, epididymides, and ductuli deferentes. As an internal control, β -actin mRNA level was measured. Relative quantification (RQ) is expressed as mean \pm standard deviation (SD). Data were obtained from 3 separate experiments. Asterisks indicate statistically significant differences (* P < 0.05, ** P < 0.01, *** P < 0.001; Mann-Whitney U-test). YSS turkeys (n = 6) and WNS turkeys (n = 6). Representative western blots and relative expression of occludin (A'), ZO-1 (B'), Cx43 (C'), N- and E-cadherin (D'), and β -catenin (E') proteins in YSS and WNS testes, epididymides, and ductuli deferentes. Densitometric analysis of protein content was normalized against the corresponding β -actin. Protein levels within the WNS tissues were arbitrary set as 1. Data obtained from 3 separate analyses are expressed as mean \pm SD. Asterisks indicate statistically significant differences (* P < 0.05, ** P < 0.01, *** P < 0.001; Mann-Whitney U-test). N = 5 each for YSS and WNS tissues.

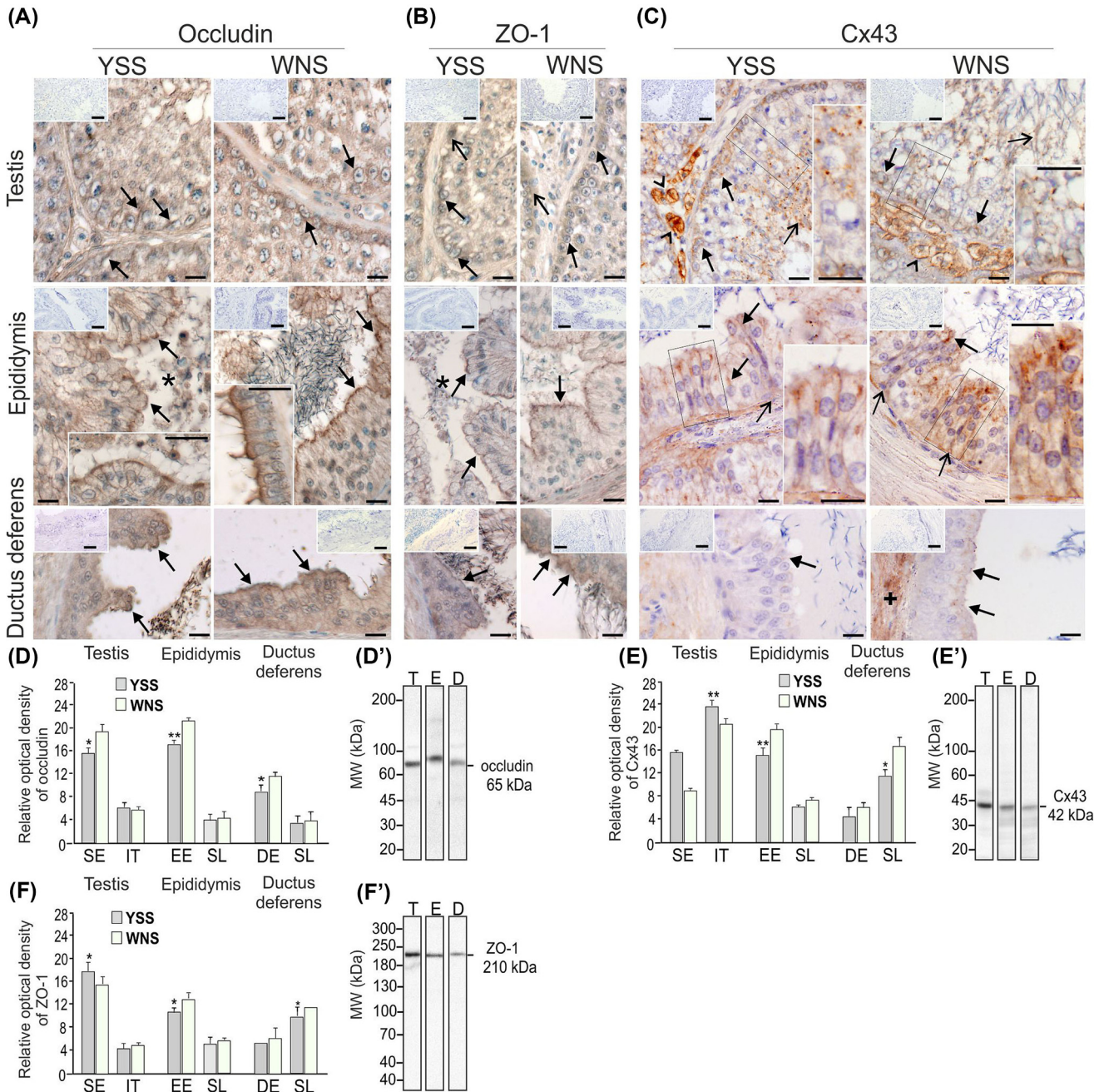


Figure 2. Qualitative (A to C) and quantitative (D to F) analysis of immunohistochemical staining for occludin (A), ZO-1 (B), and Cx43 (C). Representative micrographs from yellow semen syndrome (YSS) and white normal semen (WNS) testes, epididymides, and ductuli deferentes. Counterstaining was performed with Mayer’s haematoxylin. Scale bars are 10 μ m. Frames indicate the location of the higher magnification view. (A) Positive staining for occludin was visible in YSS and WNS testes, epididymides, and ductuli deferentes. A spoke-like pattern between Sertoli and germ cells (arrows), of discontinuous lines at the blood-epididymis barrier (BEB) (arrows), and at the apical epithelium (arrows) of YSS testis epididymis, and ductus deferens, instead of the parallel line between Sertoli and germ cells (arrows) and of the continuous lines at the luminal epithelium (arrows) of the respective WNS tissue sections were observed. Note the altered occludin staining pattern at higher magnification views (inserts in A) and reduced staining intensity in all YSS tissue sections. (B) The ZO-1 signal was either dispersed at the base of the seminiferous epithelium (open arrows) or visible in the lateral contacts between Sertoli cells (arrows) and close to the luminal border of epididymal and ductal epithelium (arrows) of YSS and WNS tissues. Note increased ZO-1 staining intensity in the YSS testis and reduced staining in YSS epididymis and ductus deferens. Note also sloughed germ cells admixed with mature spermatozoa in YSS epididymal lumen (asterisks in A and B). (C) Punctate pattern of Cx43 was visible in the basal and adluminal compartment of the testis (arrows and open arrows, respectively), while a strong, linear pattern was present between neighboring Leydig cells in the interstitial tissue (arrowheads). In the epididymal epithelium, the signal was observed between principal cells (arrows) and principal and basal cells (open arrows). Note a mixed Cx43 pattern of foci or lines at the higher magnification views. In the ductus deferens, weak Cx43 signal was seen in the YSS apical epithelium (arrows) and strong staining was observed in the WNS stroma layer (cross). Note increased Cx43 staining intensity in the YSS testis and reduced intensity in YSS epididymis and ductus deferens. (D to F) Histograms of occludin (D), ZO-1 (E), and Cx43 (F) staining intensity expressed as relative optical density (ROD) of diaminobenzidine brown reaction product. Data are expressed as mean \pm SD of 3 independent experiments (each in triplicate). Significant differences from WNS values are denoted as * $P < 0.05$, ** $P < 0.01$. (D'-F') Immunoblots that show the specificity of the respective antibodies against occludin (D'), ZO-1 (E'), and Cx43 (F') in tissue lysates (50 μ g protein). The relative position of the protein band corresponding to the ColorBurst Electrophoresis Marker (Sigma-Aldrich) is noted to the left. Abbreviations: T – testis, E – epididymis, D – ductus deferens, SE – seminiferous epithelium, IT – interstitial tissue, EE – epididymal epithelium, DE – ductal epithelium, SL – stroma layer, MW – molecular weight.

occludin immunoreactivity appeared as a discreet, discontinuous band at the apical epithelium (Figure 2A). In all YSS reproductive tissues, changes in the staining pattern and orientation of occludin were accompanied by a reduction in the immunostaining intensity as confirmed by optical density quantitative measurement (Figure 2D). The signal was significantly reduced ($P < 0.05$) in YSS vs. WNS tissues. In the epididymal epithelium, the difference between YSS and WNS samples was even more pronounced ($P < 0.01$).

ZO-1 staining was frequently dispersed throughout the Sertoli cell cytoplasm at the base of the epithelium in both WNS and YSS testes. However, in the latter, a diffuse staining pattern colocalized with ZO-1 in lateral contacts between adjacent Sertoli cells perpendicular to the basal lamina (Figure 2B). Such a staining pattern was also apparent between adjacent epithelial cells, close to the luminal border of YSS epididymis and ductus deferens, while in WNS samples, ZO-1 staining was diffuse and/or localized to the plasma membranes of adjacent epithelial cells (Figure 2B). Of note, staining intensity increased in YSS testes ($P < 0.05$) and decreased in the YSS excurrent duct system ($P < 0.05$) compared to the respective WNS tissues (Figure 2E).

Cx43 In both YSS and WNS testes, Cx43 signal appeared as distinct foci or lines localized in the basal compartment close to the basal lamina and in the apical compartment close to the lumen (Figure 2C). Closer examination revealed that staining occurred between adjacent Sertoli cells or between Sertoli and germ cells, as shown at higher magnification (Figure 2C). In both compartments, signal intensity was stronger in YSS compared to WNS testis. In the interstitium, Cx43 immunoreactivity was observed between neighboring Leydig cells. Further, in YSS testis, there was a very strong and linear Cx43 signal at the plasma membrane, whereas in WNS testis it was clearly reduced (Figure 2C). In YSS epididymis, Cx43 was apparent as distinct foci and/or discreet lines localized along the lateral plasma membranes of adjacent epithelial principal cells and between principal and basal cells (Figure 2C), whereas a similar staining pattern of apparently stronger intensity was observed in the respective WNS epididymis. In both YSS and WNS ductus deferens, Cx43 staining was localized to the apical cytoplasm of the columnar epithelium and the stroma layer. However, there was a significant difference in staining intensity in the stroma. Cx43 signal was apparently reduced in the YSS compared to the WNS stroma (Figure 2C). The results of quantitative evaluation of the staining intensity confirmed the immunohistochemical observations. There were significant differences between the YSS and WNS testicular interstitium, epididymal epithelium, and stromal layer, ($P < 0.01$, $P < 0.01$, and $P < 0.05$ respectively; Figure 2F).

N- and E-cadherin and β -catenin In YSS and WNS testis, N-cadherin and β -catenin signals were observed in the basal and adluminal compartment of the seminiferous epithelium (Figure 3A and B). Thor-

ough analysis revealed increased N-cadherin and decreased β -catenin intensity dispersed in the cell cytoplasm and/or in the form of discontinuous lines between Sertoli and germ cells at the BTB of YSS vs. WNS testis (Figure 3A and B; see higher magnification views). In YSS epididymis, E-cadherin was localized along the lateral plasma membranes of adjacent epithelial principal cells and between principal and basal cells (Figure 3A). β -catenin localization was similar to that of E-cadherin (Figure 3B); however, E-cadherin staining intensity was increased, while that for β -catenin was reduced in YSS vs. WNS epididymis (Figure 3A and B). Along the epididymis, staining intensity was consistently strong, as shown in inserts at higher magnification (Figure 3A and B), while stromal cells were weakly stained in both YSS and WNS epididymides (Figure 3A and B). In the pseudostratified columnar epithelium of the YSS ductus deferens, E-cadherin and β -catenin signals were mainly associated with the cell surface and localized along the lateral plasma membranes of adjacent columnar cells and between columnar and basal cells (Figure 3A and B). Of note, sloughed germ cells admixed with mature spermatozoa were observed in the lumen of YSS epididymis (Figures 2A and B and 3A and B, asterisks).

Quantitative evaluation of N- and E-cadherin and β -catenin staining reflected the qualitative results (Figure 3C and D). There was a statistically significant increase in cadherin signal in YSS testis, epididymis, and ductus deferens vs. WNS tissues ($P < 0.05$, $P < 0.01$, and $P < 0.05$, respectively). In contrast, β -catenin signals were significantly reduced in YSS compared to WNS reproductive tissues ($P < 0.001$, $P < 0.01$, and $P < 0.05$, respectively). Interestingly, compared to WNS, in YSS ductus deferens, the E-cadherin signal was significantly higher in the stromal layer ($P < 0.05$), while β -catenin was significantly reduced in the ductal epithelium ($P < 0.05$).

Negative control YSS and WNS tissue sections showed no immunopositive staining for occludin, ZO-1, Cx43, N- and E-cadherin, and β -catenin when incubation was performed without the respective primary antibodies (upper inserts of Figure 2A-C).

In summary, quantitative measurement junctional protein immunohistochemical staining confirmed qPCR (Figure 1A-E) and western blot (Figure 1A'-E') analyses and indicated pronounced expression changes in occludin, ZO-1, Cx43, N- and E-cadherin, and β -catenin in YSS vs. WNS testis, epididymis, and ductus deferens (for details, see Figures 2D-F and 3C and D). Specificity of all antibodies used for immunohistochemistry were validated by western blot, as shown in Figures 2D'-F' and 3C' and D'.

DISCUSSION

In the present study, we sought to assess the possible changes in mRNA and protein levels of the selected junctional proteins that are present at the testicular, epididymal, and ductal epithelia of YSS vs.

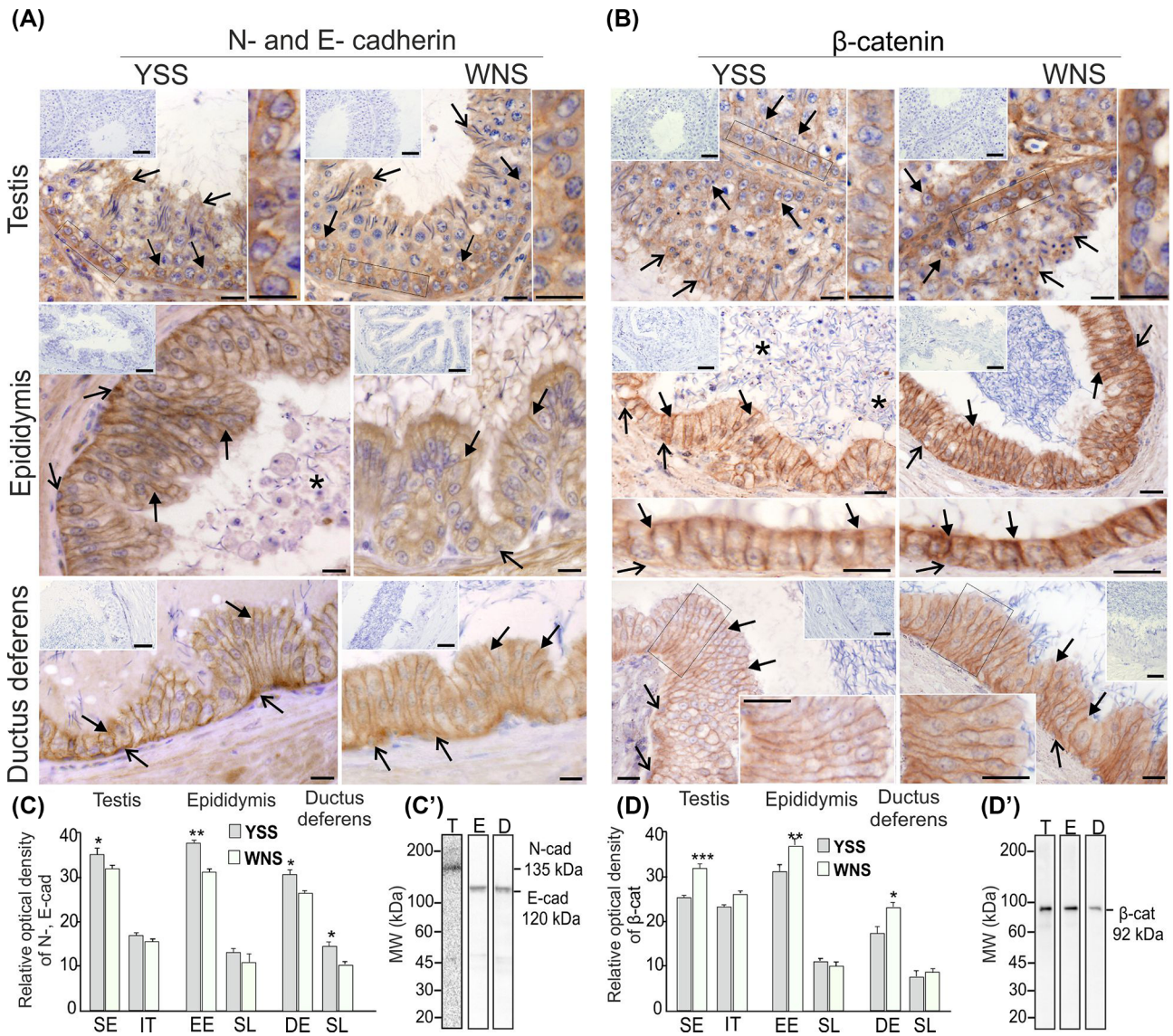


Figure 3. Qualitative (A and B) and quantitative (C and D) analysis of immunohistochemical staining for N- and E-cadherin (A) and β -catenin (B). Representative micrographs of yellow semen syndrome (YSS) and white normal semen (WNS) testes, epididymides, and ductuli deferentes. Counterstaining was performed with Mayer's haematoxylin. Scale bars are 10 μ m. Frames indicate the location of the higher magnification view. (A and B) Similar staining pattern for N- and E-cadherin (A) and β -catenin (B) were observed in the basal compartment at the blood-testis barrier (BTB) (arrows) and in the adluminal compartment of seminiferous epithelium (open arrows) as well as in the lateral plasma membranes of adjacent epididymal principal cells (arrows) and between principal and basal cells (open arrows), and in the lateral plasma membranes of adjacent ductal columnar cells (arrows) and between columnar and basal cells (open arrows) of YSS and WNS epididymides and ductuli deferentes. Note increased N- and E-cadherin and reduced β -catenin staining intensity at the BTB of YSS testis (see higher magnification views in A and B) and of YSS epididymis and ductus deferens sections (see higher magnification inserts in B). Note weaker staining for β -catenin between epithelial principal cells (arrows) and principal and basal cells (open arrows) along the entire YSS epididymis length (see higher magnification inserts in B). Note also sloughed germ cells admixed with mature spermatozoa in YSS epididymal lumen (asterisks in A and B). (C and D) Histograms of N- and E-cadherin (C) and β -catenin (D) staining intensity expressed as ROD of diaminobenzidine brown reaction product. Data are expressed as mean \pm SD of 3 independent experiments (each in triplicate). Significant differences from WNS values are denoted as * P < 0.05, ** P < 0.01, *** P < 0.001. (C'-D') Immunoblots that show the specificity of the respective antibodies against N- and E-cadherin (C') and β -catenin (D') in tissue lysates (50 μ g protein). The relative position of the protein band corresponding to the ColorBurst Electrophoresis Marker (Sigma-Aldrich) is noted to the left. Abbreviations: T – testis, E – epididymis, D – ductus deferens, SE – seminiferous epithelium, IT – interstitial tissue, EE – epididymal epithelium, DE – ductal epithelium, SL – stroma layer, MW – molecular weight.

WNS turkeys. It should be added that the molecular composition of intercellular junctions in the reproductive tissues of domestic turkey has not yet been demonstrated.

We observed downregulation of occludin mRNA and protein in all YSS reproductive tissues. These results

coincide well with altered occludin immunostaining patterns found at the BTB of YSS testis and the BEB region of YSS epididymis. It should be stressed that in YSS epididymis such an altered expression pattern was observed along the entire tissue length (compare higher magnification micrographs in Figure 2A). Both findings

clearly indicate impaired functionality of reproductive epithelia in YSS turkeys.

It is tempting to speculate that changes in ZO-1 and Cx43 expression in YSS reproductive tissues may also contribute to disturbed functionality. This notion is supported by the following observations: increased ZO-1 and Cx43 mRNA and protein expression in YSS testis and reduced expression of these proteins in YYS epididymis and ductus deferens as compared to the respective WNS tissue. Moreover, similar expression patterns of both junctional proteins may indicate a possible relationship between ZO-1 and Cx43 expression in turkey reproductive tissues. Similar physical association of Cx43 with ZO-1 as well as ZO-1-regulated gap junction organization was reported in cardiac myocytes (Toyofuku et al., 1998), osteoblastic cells (Laing et al., 2001), and Sertoli cells (Segretain et al., 2004). It is relevant to note that altered ZO-1 localization was also observed in rat testes exposed to various toxicants (Wong et al., 2004; Sobarzo et al., 2009) that led to the loss of functional BTB integrity as a consequence of ZO-1 protein mislocalization.

In turkey testes, Cx43 signal was observed at the BTB in the basal epithelium and between Sertoli and germ cells in the adluminal compartment, more precisely at the Sertoli cell-elongated spermatid interface. Interestingly, the staining intensity at the BTB was stronger in YSS compared to WNS tissue. Increased Cx43 immunoexpression at the BTB of YSS testis may result, at least partly, from increased ZO-1 expression in this region. A similar relationship between impaired Cx43 and ZO-1 protein distribution at the BTB was demonstrated in adult rat testis exposed to flutamide (Chojnacka et al., 2016). It should be noted that elevated Cx43 mRNA and protein in YSS testis are presumably caused by increased Cx43 expression in the interstitial space, as shown by quantitative analysis of immunohistochemical staining. This pattern may reflect disturbed functionality of YSS Leydig cells, as reported in our previous study (Pardyak et al., 2018) that showed increased testosterone and estradiol concentrations in YSS vs. WNS testes. It is interesting to note here that the absence or apparent decrease of Cx43 expression within seminiferous tubules, and the loss of Cx43 from Sertoli cells in rodents and humans with impaired testis functionality, results in Leydig cell hyperplasia (Kotula-Balak et al., 2007; for review see Kidder and Cyr, 2016).

As reported earlier (Fiorini et al., 2004; Brehm et al., 2007), Cx43 represents a functional marker for Sertoli cells and contributes to coexisting tight and adherens junctions to organize the BTB. To date, however, the physiological role of Cx43-mediated gap junctions in processes that involve the final maturation of spermatozoa during their transit along the epididymal duct is not fully elucidated, although gap junctions between adjacent principal cells of rat epididymis were identified by freeze-fracture electron microscopy in 1972 (Friend and Gilula, 1972). It is possible that reduced Cx43 expression in the BEB and between the principal and basal

cells might lead to altered epithelial integrity and disturbed cellular homeostasis in YSS epididymis (Cyr, 2011; Kidder and Cyr, 2016). More than ten years ago, the Cyr group demonstrated that the BEB is critical for the maintenance and composition of the luminal environment in the epididymal duct (Cyr et al., 2007). Interestingly, analysis of male reproductive function in mice with mutations in *Cx43* revealed that spermatozoa quality and motility in mutant mice were significantly decreased while epididymal morphology was not altered (Gregory et al., 2011).

Further, strong Cx43 staining in the WNS ductus deferens stromal cells may indicate a putative role of connective tissue cells in the cell-to-cell communication that mediates signals to the excurrent duct epithelium. If this conjecture is true, a distinct reduction of the Cx43 signal in the YSS stroma may suggest an adverse impact on direct intercellular communication and exchange of small growth-regulatory molecules that are indispensable for the luminal microenvironment and, consequently, proper sperm maturation. This supposition agrees with the widely accepted idea that expression and localization of connexins are altered during cellular distress, related to disease or chemical insult, and lead to abnormal intercellular communication (for further details see Mesnil et al., 2005).

Finally, our results suggest that adherens junction-constituent protein levels might influence the ductus epididymis lumen microenvironment in YSS turkeys. We detected upregulation of *N-* and *E-cadherin* and downregulation of *β -catenin* genes in YSS testis and excurrent duct system compared to the respective WNS tissues. N-cadherin is expressed in the seminiferous epithelium, whereas E-cadherin is present in excurrent duct epithelia (Cyr et al., 1993; Andersson et al., 1994). Here, we found that N-cadherin and *β -catenin* distribution in YSS testis was altered predominantly at the BTB region (compare higher magnification micrographs in Figure 3A and B), and this finding may suggest dysregulated trafficking or enhanced endocytosis of the adherens junction proteins (Fiorini et al., 2008; Li et al., 2009). A significant increase in E-cadherin and decrease in the *β -catenin* staining in the YSS excurrent duct, as detected by immunohistochemistry, supports this hypothesis. The above results are in line with the idea that affected fertility in domestic poultry might be associated with epididymal abnormalities (Deviche et al., 2011) and our observation that sloughed germ cells (admixed with mature spermatozoa) and dense epididymal fluid were present in the lumen of the epididymis of YSS turkey.

Taken together, the most prominent alterations in cell-cell junction protein gene expression, their distribution, and the staining intensity were observed in YSS epididymis and ductus deferens compared to WNS tissues. The gene and protein expression data from tissue homogenates were confirmed by subcellular distribution of occludin, ZO-1, Cx43, N- and E-cadherin, and *β -catenin* in YSS reproductive tissue samples, as

visualized with light microscopy. In our previous study, we reported a positive correlation between quantitatively measured immunolocalization and expression of junction proteins in the rat (Zarzycka et al., 2015). The present results are the first that demonstrate altered levels of junctional protein mRNA and protein expression could be related to the appearance of yellow semen in domestic turkeys.

ACKNOWLEDGMENTS

Supported by a grant PRELUDIUM13, 2017/25/N/NZ9/00585 from the National Science Centre.

REFERENCES

- Andersson, A. M., K. Edvardsen, and N. E. Skakkebaek. 1994. Expression and localization of N- and E-cadherin in the human testis and epididymis. *Int. J. Androl.* 17:174–80.
- Banerjee, S., and C. M. Chaturvedi. 2018. Simulated photoperiod influences testicular activity in quail via modulating local GnRHR-GnIHR, GH-R, Cnx-43 and 14-3-3. *J. Photochem. Photobiol. B.* 178:412–423.
- Bergmann, M., J. Schindelmeiser, and H. Greven. 1984. The blood-testis barrier in vertebrates having different testicular organization. *Cell Tissue Res.* 238:145–150.
- Bilinska, B., A. Hejmej, and M. Kotula-Balak. 2018. Preparation of testicular samples for histology and immunohistochemistry. Pages 17–36 in *Sertoli cell: Methods and Protocols*, M. Alves, and P. F. Oliveira, eds. Springer Science+Business Media, Humana Press, New York, NY 10013, USA.
- Bordeaux, J., A. W. Welsh, S. Agarwal, E. Killiam, M. T. Baquero, J. A. Hanna, Y. K. Anagnostou, and D. L. Rimm. 2010. Antibody validation. *Biotechniques.* 48:197–209.
- Brehm, R., M. Zeiler, C. Rüttinger, K. Herde, M. Kibschull, E. Winterhager, K. Willecke, F. Guillou, C. Lécureuil, K. Steger, L. Konrad, K. Biermann, K. Failing, and M. Bergmann. 2007. A Sertoli cell specific knockout of connexin43 prevents initiation of spermatogenesis. *Am. J. Pathol.* 171:19–31.
- Carreau, S., and R. A. Hess. 2010. Oestrogens and spermatogenesis. *Philos. Trans. R. Soc. Lond. B Biol. Sci.* 365:1517–1535.
- Cheng, C. Y., and D. D. Mruk. 2002. Cell junction dynamics in the testis: Sertoli-germ cell interactions and male contraceptive development. *Physiol. Rev.* 82:825–874.
- Chojnacka, K., A. Hejmej, M. Zarzycka, W. Tworzydło, S. M. Bilinski, L. Pardyak, A. Kaminska, and B. Bilinska. 2016. Flutamide induces alterations in the cell-cell junction ultrastructure and reduces the expression of Cx43 at the blood-testis barrier with no disturbance in the rat seminiferous tubule histology. *Reprod. Biol. Endocrinol.* 14:14.
- Cyr, D. G., B. Robaire, and L. Hermo. 1995. Structure and turnover of junctional complexes between principal cells of the rat epididymis. *Microsc. Res. Tech.* 30:54–66.
- Cyr, D. G., M. Gregory, E. Dube, J. Dufresne, P. T. K. Chan, and L. Hermo. 2007. Orchestration of occludins, catenins and cadherins as players involved in maintenance of the blood-epididymal barrier in animals and humans. *Asian J. Androl.* 9:463–475.
- Cyr, D. G. 2011. Connexins and pannexins: coordinating cellular communication in the testis and epididymis. *Spermatogenesis.* 1:325–338.
- Cyr, D. G., L. Hermo, and B. Robaire. 1993. Developmental changes in epithelial cadherin messenger ribonucleic acid and immunocytochemical localization of epithelial cadherin during postnatal epididymal development in the rat. *Endocrinology.* 132:1115–1124.
- Deviche, P., L. L. Hurley, and H. B. Fokidis. 2011. Avian testicular structure, function, and regulation. Pages 27–70 in *Hormone and Reproduction in Vertebrates. Vol. 4. Birds*. D. Norris, and K. H. Lopez, eds. Academic Press.
- Fiorini, C., J. Gilleron, D. Carette, A. Valette, A. Tilloy, S. Chevalier, D. Segretain, and G. Pointis. 2008. Accelerated internalization of junctional membrane proteins (connexin 43, N-cadherin and ZO-1) within endocytic vacuoles: an early event of DDT carcinogenicity. *Biochim. Biophys. Acta.* 1778:56–67.
- Fiorini, C., A. Tilloy-Ellul, S. Chevalier, C. Charuel, and G. Pointis. 2004. Sertoli cell junctional proteins as early targets for different classes of reproductive toxicants. *Reprod. Toxicol.* 18:413–421.
- Friend, D. S., and N. B. Gilula. 1972. Variations in tight and gap junctions in mammalian tissue. *J. Cell Biol.* 53:758–776.
- Goossens, S., and F. van Roy. 2005. Cadherin-mediated cell-cell adhesion in the testis. *Front. Biosci.* 10:398–419.
- Gorowska, E., K. Chojnacka, M. Zarzycka, B. Bilinska, and A. Hejmej. 2014. Postnatal exposure to flutamide affects *CTNNB1* and *CDH1* gene expression in adult pig epididymis and prostate and alters metabolism of testosterone. *Andrology.* 2:186–197.
- Gregory, M., C. N. Kahiri, K. J. Barr, C. E. Smith, L. Hermo, D. G. Cyr, and G. M. Kidder. 2011. Male reproductive system defects and subfertility in a mutant mouse model of oculodentodigital dysplasia. *Int. J. Androl.* 34:e630–641.
- Hejmej, A., and B. Bilinska. 2018. The effects of flutamide on cellular junctions in the testis and epididymis and prostate. *Reprod. Toxicol.* 81:1–16.
- Hejmej, A., I. Kopera, M. Kotula-Balak, M. Lydka, M. Lenartowicz, and B. Bilinska. 2012. Are expression and localization of tight and adherens junction proteins in testes of adult boar affected by fetal and neonatal exposure to flutamide? *Int. J. Androl.* 35:340–352.
- Hess, R. A., and R. J. Thurston. 1984. Detection and incidence of yellow turkey semen on commercial breeder farms. *Poult. Sci.* 10:2084–2086.
- Hess, R. A., R. J. Thurston, and H. V. Biellier. 1976. Morphology of the epididymal region and ducts deferens of the turkey (*Meleagris gallopavo*). *J. Anat.* 122:241–252.
- Hess, R. A., R. J. Thurston, and H. V. Biellier. 1982. Morphology of the epididymal region of turkeys producing abnormal yellow semen. *Poult. Sci.* 61:531–539.
- Hess, R. A., D. Bunick, and J. Bahr. 2001. Oestrogen, its receptors and function in the male reproductive tract - a review. *Mol. Cell. Endo.* 178:29–38.
- Izzo, G., M. d'Istria, D. Ferrara, I. Serino, F. Aniello, and S. Minucci. 2006. Connexin 43 expression in the testis of the frog *Rana esculenta*. *Zygote.* 14:349–57.
- Kidder, G. M., and D. G. Cyr. 2016. Roles of connexins in testis development and spermatogenesis. *Semin. Cell Develop. Biol.* 50:22–30.
- Kopera, I., B. Bilinska, C. Y. Cheng, and D. D. Mruk. 2010. Sertoli-germ cell junctions in the testis - a review of recent data. *Phil. Trans. R. Soc. Lond. B Biol. Sci.* 365:1593–1605.
- Kotula-Balak, M., A. Hejmej, J. Sadowska, and B. Bilinska. 2007. Connexin 43 expression in human and mouse testes with impaired spermatogenesis. *Eur. J. Histochem.* 51:261–268.
- Kotula-Balak, M., R. Zielinska, J. Glogowski, R. K. Kowalski, B. Sarosiek, and B. Bilinska. 2008. Aromatase expression in testes of XY, YY, and XX rainbow trout (*Oncorhynchus mykiss Walbaum*). *Comp. Biochem. Physiol. Part A, Mol. Integrat. Physiol.* 149:188–196.
- Laing, J. G., R. N. Manley-Markowski, M. Koval, R. Civitelli, and T. H. Steinberg. 2001. Connexin45 interacts with zonula occludens-1 and connexin43 in osteoblastic cells. *J. Biol. Chem.* 276: 23051–23055.
- Levy, S., and B. Robaire. 1999. Segment-specific changes with age in the expression of junctional proteins and the permeability of the blood-epididymis barrier in rats. *Biol. Reprod.* 60:1392–1401.
- Li, M. W., D. D. Mruk, W. M. Lee, and C. Y. Cheng. 2009. Disruption of the blood-testis barrier integrity by bisphenol A in vitro: is this a suitable model for studying blood-testis barrier dynamics? *Int. J. Biochem. Cell. Biol.* 41:2302–2314.
- Livak, K. J., and T. D. Schmittgen. 2001. Analysis of relative gene expression data using real-time quantitative PCR and the 2(-delta delta C(T)) method. *Methods.* 25:402–408.

- Mesnil, M., S. Crespin, J. L. Avanzo, and M. L. Zaidan-Dagli. 2005. Defective gap junctional intercellular communication in the carcinogenic process. *Biochim. Biophys. Acta.* 1719:125–145.
- Mital, P., B. T. Hinton, and J. M. Dufour. 2011. The blood-testis and blood-epididymis barriers are more than just their tight junctions. *Biol. Reprod.* 84: 851–858.
- Mruk, D. D., and C. Y. Cheng. 2015. The mammalian blood-testis barrier: its biology and regulation. *Endocr. Rev.* 36: 564–591.
- Mruk, D. D., and C. Y. Cheng. 2010. Tight junctions in the testis: new perspectives. *Phil. Trans. R. Soc. Lond. B Biol. Sci.* 365:1621–1635.
- Mruk, D. D., and C. Y. Cheng. 2004. Sertoli-Sertoli and Sertoli-germ cell interactions and their significance in germ cell in the seminiferous epithelium during spermatogenesis. *Endocr. Rev.* 25:747–806.
- O'Donnell, L., K. M. Robertson, M. E. Jones, and E. R. Simpson. 2001. Estrogen and spermatogenesis. *Endocrin. Rev.* 22:289–318.
- Osman, D. I., H. Ekwall, and L. Ploen. 1980. Specialized cell contacts and the blood-testis barrier in the seminiferous tubules of the domestic fowl (*Gallus domesticus*). *Int. J. Androl.* 3: 553–562.
- Pardyak, L., A. Kaminska, M. Brzoskwinia, A. Hejmej, M. Kotula-Balak, J. Jankowski, A. Ciereszko, and B. Bilinska. 2018. Differences in aromatase expression and steroid hormone concentrations in the reproductive tissues of male domestic turkeys (*Meleagris gallopavo*) with white and yellow semen. *Br. Poult. Sci.* 59:591–603.
- Pelletier, R. M. 1990. A novel perspective: the occluding zonule encircles the apex of the Sertoli cell as observed in birds. *Am. J. Anat.* 188:87–108.
- Pointis, G., J. Gilleron, D. Carette, and D. Segretain. 2010. Physiological and physiopathological aspects of connexins and communicating gap junctions in spermatogenesis. *Phil. Trans. R. Soc. Lond. B Biol. Sci.* 365:1607–1620.
- Robaire, B., and R. S. Viger. 1995. Regulation of epididymal epithelial cell functions. *Biol. Reprod.* 52:226–236.
- Rowlands, T. M., J. M. Symonds, R. Farookhi, and O. Blaschuk. 2000. Cadherins: crucial regulators of structure and function in reproductive tissues. *Rev. Reprod.* 5:53–61.
- Saez, J. C., V. M. Berthoud, M. C. Branes, A. D. Martinez, and E. C. Bneyer. 2003. Plasma membrane channels formed by connexins: their regulation and functions. *Physiol. Rev.* 83: 1359–400.
- Segretain, D., C. Fiorini, X. Decrouy, N. Defamie, J. R. Prat, and G. Pointis. 2004. A proposed role for ZO-1 in targeting connexin 43 gap junctions to the endocytic pathway. *Biochimie.* 86:241–44.
- Sharpe, R. M. 1998. The roles of oestrogen in the male. *Trends Endocrinol. Met.* 9:371–377.
- Slowinska, M., J. Jankowski, M. Dietrich, H. Karol, E. Liszewska, J. Glogowski, K. Kozłowski, K. Sartowska, and A. Ciereszko. 2011. Effect of organic and inorganic forms of selenium in diets on turkey semen quality. *Poult. Sci.* 90:181–190.
- Slowinska, M., K. Kozłowski, J. Jankowski, and A. Ciereszko. 2015. Proteomic analysis of white and yellow seminal plasma in turkeys (*Meleagris gallopavo*) seminal plasma. *J. Anim. Sci.* 93:2785–2795.
- Slowinska, M., E. Liszewska, J. Nynca, J. Bukowska, A. Hejmej, B. Bilinska, J. Szubstarski, K. Kozłowski, J. Jankowski, and A. Ciereszko. 2014. Isolation and characterization of ovoinhibitor, a multidomain kazal-like inhibitor from turkey (*Meleagris gallopavo*) seminal plasma. *Biol. Reprod.* 91:1–15.
- Smolen, A. J. 1990. Image analytic techniques for quantification of immunocytochemical staining in the nervous system. Pages 208–229 in *Methods in Neurosciences*. P. M. Conn, ed. Academic Press, San Diego, CA.
- Sobarzo, C. M., L. Lustig, R. Ponzio, M. O. Suescun, and B. Denduchis. 2009. Effects of di(2-ethylhexyl) phthalate on gap and tight junction protein expression in the testis of prepubertal rats. *Microsc. Res. Tech.* 72:868–877.
- Thurston, R. J., and N. Korn. 1997. Semen quality in the domestic turkey: the yellow semen syndrome. *Avian Poult. Biol. Rev.* 8:109–121.
- Thurston, R. J., R. A. Hess, D. P. Froman, and H. V. Biellier. 1982. Elevated seminal plasma proteins: a characteristic of yellow turkey semen. *Poult. Sci.* 61:1905–1911.
- Toyofuku, T., M. Yabuki, K. Otsu, T. Kuzuya, M. Hori, and M. Tada. 1998. Direct association of the gap junction protein connexin-43 with ZO-1 in cardiac myocytes. *J. Biol. Chem.* 273:12725–12731.
- Wong, C. H., D. D. Mruk, W. Y. Lui, and C. Y. Cheng. 2004. Regulation of blood-testis barrier dynamics: an in vivo study. *J. Cell Sci.* 117:783–798.
- Wong, C. H., and C. Y. Cheng. 2005. The blood-testis barrier: its biology, regulation, and physiological role in spermatogenesis. *Curr. Top. Dev. Biol.* 71:263–296.
- Zarzycka, M., K. Chojnacka, D. D. Mruk, E. Gorowska, A. Hejmej, M. Kotula-Balak, L. Pardyak, and B. Bilinska. 2015. Flutamide alters distribution of c-Src and affects cell adhesion function in the adult rat seminiferous epithelium. *Andrology.* 3:569–581.